Published in the Slovak Republic
European Journal of Molecular Biotechnology
Has been issued since 2013.
E-ISSN: 2409-1332
2020, 8(1): 3-13

DOI: 10.13187/ejmb.2020.1.3
www.ejournal8.com

Articles

Quantum Mechanical Descriptors of Π-Conjugated Imidazolinone Compounds: A DFT Study

Abdelkhalk Aboulouard [a], Ali Barhoumi [b], Abdellah Zeroual [b], Abdessamad Tounsi [c], Mohammed El idrissi [a, *]

[a] Sultan Moulay Slimane University, Beni Mellal, Morocco
[b] Chouaïb Doukkali University, El Jadida, Morocco
[c] Research Team in Applied Chemistry and Modeling ERCAM, Beni-Mellal, Morocco

Abstract

In this work, natural bond orbital (NBO) analysis, nonlinear optical and the thermodynamic properties of six organic π-conjugated compounds based on imidazolinone have been analyzed by employing density functional theory (DFT) level employing B3LYB/6-31G (d, p) basis set. NBO analysis reveals that the intra-intermolecular charge transfer occurs within the molecules leading to the stabilization. The predicted nonlinear optical (NLO) properties like; polarizability and first hyperpolarizabiliy support showed that the six organic π-conjugated studied imidazolone derivatives compounds could attract the interests for future investigation. The LUMO energy is increasingly concentrated around the nitrogen group of the chain by the acceptor groups with the increase of their mesomeric attractor effect in the following order – P6 < P1 < P4 < P5 < P3 < P2-. This explains the decrease in gap energy ΔE(P2) > ΔE (P3)> ΔE (P5) > ΔE (P4) > ΔE(P1)> ΔE(P6).

Keywords: imidazolinone, DFT, B3LYB, NBO, NLO, nonlinear optical, polarizability, hyperpolarizabiliy.

1. Introduction

Over recent years, imidazolinones have gained much attention due to their environmentally friendly molecular properties. Imidazolinones have been used to study the solar cell activity (Sharma, Handique, 2016). Moreover, imidazolinones are well known for their optoelectronic, biological, pharmacological and photochemical properties (Chuang et al., 2009; Bhattacharjya et al., 2008; Bahadur, Srivastava, 2004; You et al., 2000). In this study, NLO analysis of the studied molecules were evaluated at the B3LYP basis set. The chemical descriptors such as the Polarizability (α), anisotropic (Δα), polarizability (β), hyperpolarizability <β> and isotropic β// were computed using the TD-DFT method. Furthermore, NBO analysis were examined with DFT/B3LYB, CAM-B3LYP, HSEH1PBE, HCTH407 and WB97XD basis set (Bahçeli et al., 2015).

The most used photovoltaic technology is silicon solar cell which is considered as inorganic ones (Kim et al., 2005). The disadvantages of silicon solar cells are their price and complicated fabrication procedures. Due to such disadvantages, a new generation of solar cells has been emerged. This includes organic solar cells (OSCs) (Yang et al., 2005; Park et al., 2009), perovskite

* Corresponding author
E-mail addresses: m.elidrissi2018@gmail.com (M. El idrissi)

solar cells (Green et al., 2009; Lee, 2007) dye sensitized solar cells (Hadipour, 2008; Ameri, 2009), quantum dots solar cells (Boreland, 2008; Lu et al., 2015).

2. Materials and methods

All geometry optimizations computation was executed using the Gaussian 09 programs (Frisch et al., 2009). The geometries of the products were fully optimized through DFT calculations using the B3LYP functional (Becke, 1993; Yang, 1988), jointly in addition to the 6-311G (d,p) basis set (Francl, 1982). Initial structures were cleaned repeatedly to obtain normalized geometry. Each of the P1 and P2 was then subjected for successive optimization using DFT methods in conjunction with appropriate basis sets. Final optimization of these molecules is achieved using DFT/B3LYP/6-311G (d, p) method. Final optimization of these molecules is achieved using DFT/B3LYP/6-311G (d, p) method. For computation of linear and NLO properties, the additional key of "optical" was included in the study. Following equations are used for the extraction of parameters and properties of these impurities. Molecular complexity is the criterion that can be related with Δα (Chen et al., 2017; Aihara et al., 1999; Obot et al., 2009; Ghanadzadeh et al., 2000). More the complexity of structure more is the anisotropy of polarizability (Δα) (Zhan et al., 2003; Xue et al., 2004).

While dipole moment (DM) is the measure of α of a molecule in its ground state, α is the intrinsic capacity of a molecule of having a dipole when it is assaulted with an external electric field (Harris et al., 1999; Lim et al., 1999). If a molecule is present in a weak, static electric field (of strength, F), then the total energy (E) of the molecule can be express as a Taylors series.

$$E_F = E_0 - \mu_\alpha F_\alpha - \frac{1}{2!}\alpha_{\alpha\beta}F_\alpha F_\beta - \frac{1}{3!}\alpha_{\alpha\beta\gamma}F_\alpha F_\beta F_\gamma - \frac{1}{3!}\alpha_{\alpha\beta\gamma\delta}F_\alpha F_\beta F_\gamma F_\gamma \dots\dots\dots (1)$$

E0 denotes the energy of the molecule in the absence of an external electrical field. Energy (E_o), dipole moment (μ_α), polarizability (ααβ), and first- and second-order hyperpolarizability (βαβγ and γαβγδ, respectively) denote the molecular properties. First polarizability and second hyperpolarizabilities are expressed as tensor quantities, whereas subscripts single, double, etc., denote the first-rank and second-rank tensor, etc., in Cartesian coordinate (Desharnais et al., 2003).

If the external field lies on any one of the three orthogonal Cartesian axes, then the components of the induced moments will be parallel to the field. In that case, off-diagonal terms of the tensor, ααβ vanish. Under these conditions, the expected value of αand DM obtained as:

$$DM = \sqrt{(\mu_X^2 + \mu_Y^2 + \mu_Z^2)} \quad Or \quad <\alpha_{STATIC}> = \frac{(\alpha_{XX} + \alpha_{YY} + \alpha_{ZZ})}{3} \qquad (2)$$

In case of the anisotropic orientation of the external field, the anisotropy of the polarizability (<Δα>) can be computed as:

$$<\Delta\alpha> = \left[\frac{(\alpha_{XX} - \alpha_{YY})^2 + (\alpha_{YY} - \alpha_{ZZ})^2 + (\alpha_{YY} - \alpha_{ZZ})^2 + 6(\alpha_{XX}^2 - \alpha_{XY}^2 + \alpha_{YZ}^2)^2}{2}\right]^{\frac{1}{2}} \qquad (3)$$

Similarly, the first-order (βαβγ) and second-order (γαβγδ) hyperpolarizability is calculated from components of respective tensors that are obtained from the Gaussian 09 output file.

$$\left\{ \begin{array}{c} <\alpha_{STATIC}> = (\beta_X^2 + \beta_Y^2 + \beta_{XZ}^2)^{\frac{1}{2}} \\ \beta_i = \beta_{iii} + \frac{1}{3}\sum_{i\neq k}(\beta_{ikk} + \beta_{kik} + \beta_{kki}) \\ <\alpha_{STATIC}> = \left[\sqrt{\begin{array}{c}(\beta_{XXX} + \beta_{XYY} + \beta_{XZZ})^2 + (\beta_{YYY} + \beta_{YZZ} + \beta_{YXX})^2 \\ + (\beta_{ZZZ} + \beta_{ZXX} + \beta_{ZYY})^2\end{array}}\right] \end{array} \right\} \qquad (4)$$

$$<\alpha_{STATIC}> = \frac{\gamma_{XXXX} + \gamma_{YYYY} + \gamma_{ZZZZ} + 2\gamma_{YYXX} + 2\gamma_{YYZZ} + 2\gamma_{ZZXX}}{5} \qquad (5)$$

All these optical terms have been calculated using appropriate basis set that contains polarized and diffused functions for high accuracy, in that DFT/B3LYP/6-311G (d, p) was preferred.

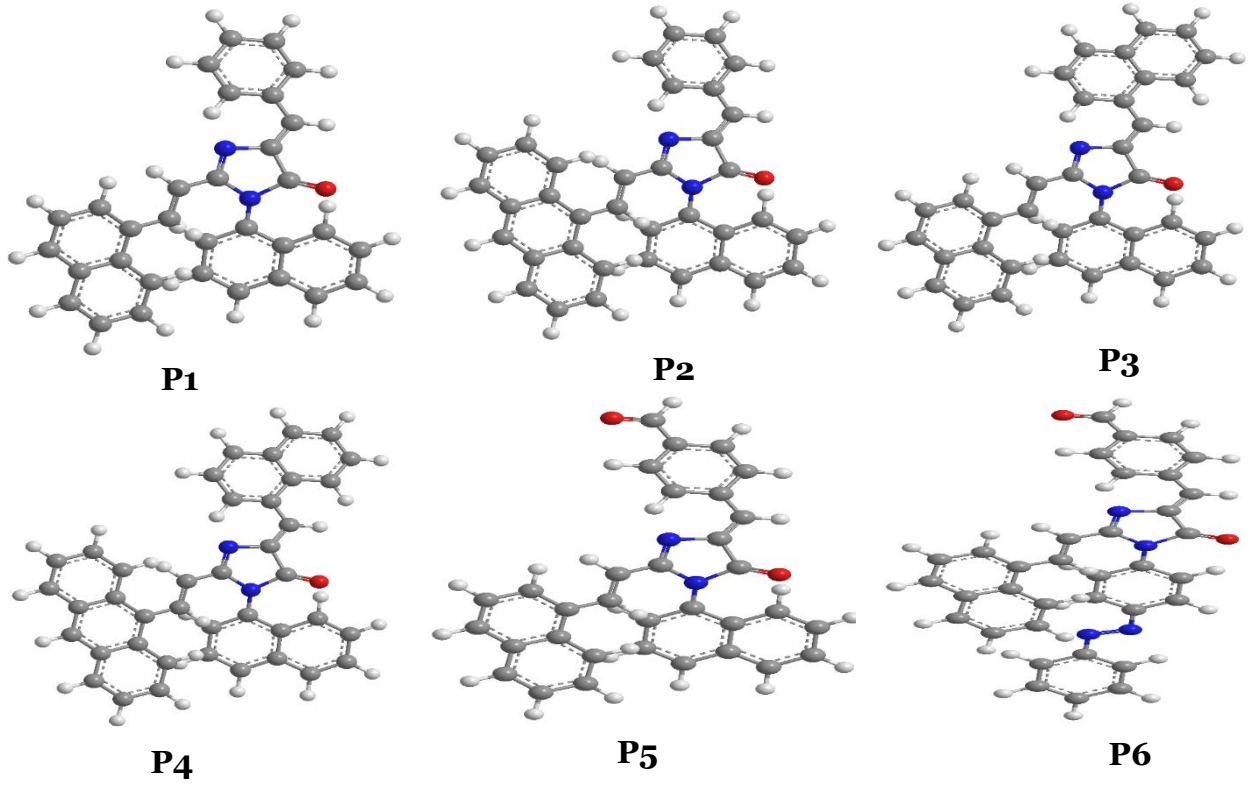

Fig. 1. Chemical structure of studied compounds

3. Results and discussion

The highest occupied molecular orbital (HOMO) and lowest unoccupied molecular orbital (LUMO) for P1 to P6 imidazolone derivatives are presented in (Figure 1), along with their optimized structures. While HOMO delocalizes over bonds of P1, and P2, it is less prominent for P1 to P6. Notably, the delocalization is uniform in P1. By the use of DFT/B3LYP/6-311G (d, p) level of theory, the extracted energies for HOMO, LUMO, and ΔE for P1 and P2 are presented in (Table 1) and compared in (Figure 2).

Table 1. HOMO, LUMO, and band gap energies for P1 to P6 imidazolone derivatives. The band gap is computed by $E_{LUMO} - E_{HOMO}$

Compounds	HOMO (eV)	LUMO (eV)	Band gap (eV)
P1	-4.028	-2.852	1.178
P2	-5.358	-3.011	2.347
P3	-5.082	-3.074	2.008
P4	-4.009	-2.815	1.194
P5	-4.291	-3.059	1.232
P6	-4.328	-3.243	1.085

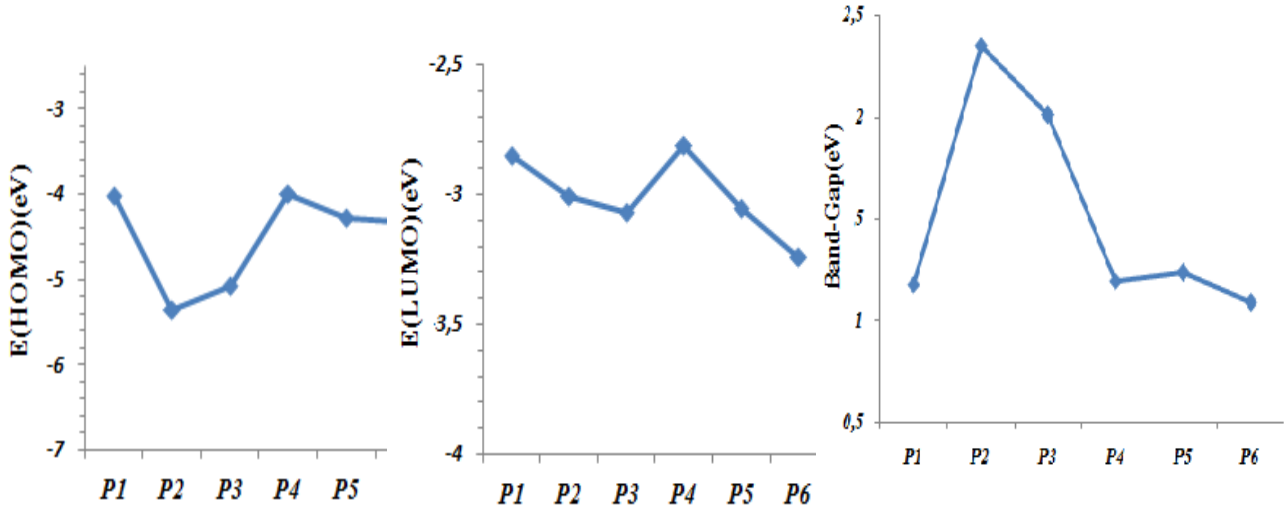

Fig. 2a **Fig. 2b** **Fig. 2c**

Fig. 2. Plot of highest occupied molecular orbitals, lowest unoccupied molecular orbitals, and band gap energies for P1 to P6

According to the Table 1, the gap energies increase from P6 to P2. This is due to the force of various acceptor groups given to the acceptor electron. Also, the HOMO/LUMO energies levels in consonance with the donor/acceptor of their electron are affected by the structure modification.

As mentioned previously, the HOMO and LUMO energies levels and band gap energies affect the photovoltaic performance of organic solar cells. The values of these energies levels are summarized in Table 1. The computational values of gap energies range from 1.085 to 2.347 eV.

It is clear from the Table 1 and Figure 2 that electron donating ability (E_{HOMO}) follows the order as P2 < P3 < P6 < P5 < P1 < P4 (Figure 2a).

Electron-accepting ability (E_{LUMO}) is seen to follow the order as P6 < P3 < P5 < P2 < P4 < P1 (Figure 2b).

What about the band gap from product P1to P6?

The chemical reactivity is highest and the kinetic stability is lowest for P6, P1 which is followed by P4, P5, P3 and P2 (Figure 2c). These proprieties are interesting to realize organic solar cells Hetero Junction.

Nonlinear optical (NLO) of P1 to P6

Intermolecular interactions the P1 to P6 are largely understood by DM, α, and first-order and second-order hyperpolarizability energy terms (Zhang et al., 2007), which are reliably computed by B3LYP/6-311G (d,p) level of the theory (Hurst et al., 2000; Gupta et al., 2017; El idrissi et al., 2019; Zeroual et al., 2017). How are these parameters affected for this compounds. To check this above basis set is used and dipole moments (DM), α, and first- and second-rank hyperpolarizability are determined (u.a). Isotropic DM ispresented in (Table 3).

Table 3. Cartesian components and net electric dipole moments (DM in Debye) for products P1 to P6

Names	DMx	DMy	DMz	DM_{Total}
P1	0.00	0.00	8.46	8.50
P2	0.00	0.00	6.38	6.40
P3	7.65	0.00	0.00	7.70
P4	8.68	0.00	0.00	8.70
P5	0.00	0.00	7.85	7.90
P6	0.00	7.16	0.00	7.20

It is seen that the X and Y components are zero in all the cases with the Z component constituting the total *DM*. Higher and lower DM_{TOTAL} than the reported mean value are highlighted in Table 3. Here, (P4, P1, P5) and (P3, P6, P2) show higher and lower DM_{TOTAL}, respectively.

The Polarizability (α), anisotropic (Δα), polarizability (β), hyperpolarizability <β> and isotropic β// values of P1 to P6products are given in Table 4. Few of these properties are also plotted in (Figure 3) (Figure 3a for α and Δα; Figure 3b for <β> and β//).

Table 4. Polarizability (α), anisotropic (Δα), polarizability (β), hyperpolarizability <β> and isotropic β// values of compounds P1 to P6 (in 10^{-30} esu Unit).

	Parameter	P1	P2	P3	P4	P5	P6
***Polarizability α *anisotropic Δα**	**α_{xx}**	31.25	35.91	30.25	34.88	32.35	29.56
	α_{yx}	9.65	10.25	7.65	8.65	7.16	8.97
	α_{yy}	29.87	33.21	30.26	31.54	30.83	32.01
	α_{zx}	10.31	11.23	12.81	10.22	11.2	9.56
	α_{zy}	9.36	10.25	12.74	9.87	10.55	8.59
	α_{zz}	58.26	64.78	43.44	50.22	51.36	51.63
	α × 10^{-24} (esu)	39.79	44.63	34.65	38.88	38.18	37.73
	Δα	80.74	87.8	72.89	67.16	70.89	68.58
***Hyperpolarizability <β> * isotropic β//**	**βxxx**	3.08	5.22	4.82	-3.87	4.23	-3.66
	βxxy	3.56	-4.41	3.22	5.32	5.22	2.88
	βyxy	2.87	4.77	-3.65	3.43	-4.02	5.23
	βyyy	4.89	-3.47	-5.23	-4.68	3.26	3.62
	βxxz	3.44	-4.41	6.03	5.28	4.92	4.61
	βyxz	-2.36	5.06	5.22	-4.69	-3.22	3.66
	βyyz	3.29	4.19	4.81	3.65	3.51	-5.22
	βzxz	-3.24	2.74	-2.68	3.02	2.86	4.87
	βzyz	4.54	-4.14	4.12	4.11	4.23	-3.02
	βzzz	-5.89	6.89	5.83	4.69	-3.68	3.82
	<β>	13.29	18.73	16.87	14.65	13.91	7.99
	β//	4.97	1.01	5.94	4.46	5.94	2.38

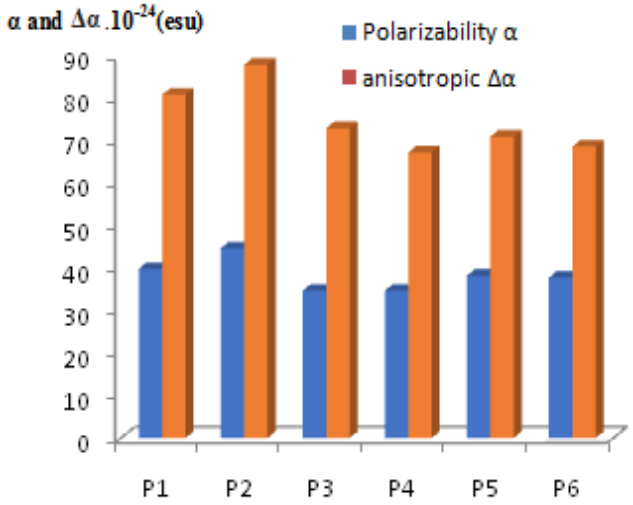

Fig. 3a

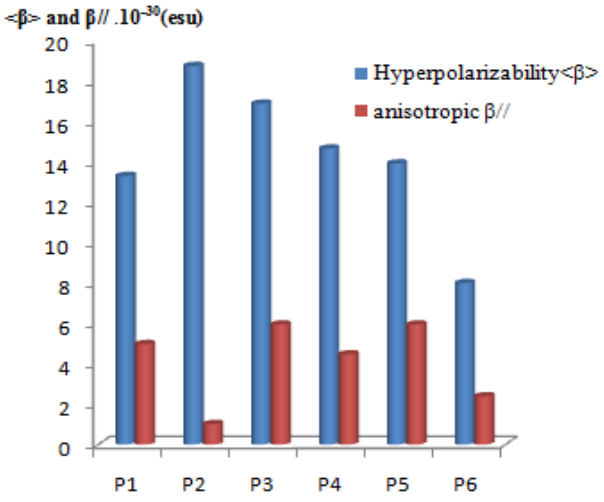

Fig. 3b

Fig. 3. Plot of polarizability (α), anisotropy of polarizability (Δα) (Figure 3a), hyperpolarizability <β> and isotropic β// (Figure 3b) for compounds P1 to P6

According to the data in (Table 1) the gap energies increase from P_6 to P_2 due to the force of various acceptor groups given to the acceptor electron. In addition, the HOMO/LUMO energy levels in agreement with the donor/acceptor of their electron are affected by the modification of the structure.

As mentioned previously, the HOMO and LUMO energies levels and band gap energies affect the photovoltaic performance of organic solar cells. The values of these energies levels are summarized in (Table 1). We can notice from these computational values of gap energies range from 1.085 to 2.347 eV.

The analysis of the results given in (Table 1) and (Figure 3) clearly shows in one hand that the electron donation capacity (EHOMO) follows the order as $P_2 < P_3 < P_6 < P_5 < P_1 < P_4$ (Figure 3a). On the other hand, the electron acceptance capacity (ELUMO) follows the order as $P_6 < P_3 < P_5 < P_2 < P_4 < P_1$ (Figure 3b).

NBO analysis

The analysis of the results obtained in the study aimed at verifying that the DFT procedure was fulfilled. On doing it previously, several descriptors associated with the results that HOMO and LUMO calculations obtained are related with results obtained using the vertical I and A following the ΔSCF procedure. A link exists between the three main descriptors and the simplest conformity to the Koopmans' theorem by linking εH with -I, ε_L with -A, and their behavior in describing the HOMO-LUMO gap as JI = $|\varepsilon_H + Egs(N-1) - Egs(N)|$, JA = $|\varepsilon_L + Egs(N) - Egs(N+1)|$ and $J_{HL}= \sqrt{J_I^2 + J_A^2}$. Notably, the JA descriptor consists of an approximation that remains valid only when the HOMO that a radical anion has (the SOMO) shares similarity with the LUMO that the neutral system has. Consequently, we decided to design an other descriptor ΔSL (the difference between the SOMO and LUMO energies), to guide in verifying how the approximation is accurate (Weigend et al., 2005; Pereira et al., 2017). The results of this analysis are presented in (Tables 5 to 10).

Table 5. Electronic energies of the neutral, positive and negative molecular systems (in au), the HOMO, LUMO, and SOMO orbital energies (in eV), JI, JA, JHL, and ΔSL descriptors (also in eV) calculated with DFT/B3LYB, CAM-B3LYP, HSEH1PBE, HCTH407 and WB97XD for compound P1

	E_o	E^+	E^-	HOMO	LUMO	SOMO	J_i	J_A	J_{HL}	ΔS_L
B3LYP	-1402.064	-1401.654	-1402.458	-4.028	-2.852	-3.885	14.748	14.008	20.341	1.033
CAM-B3LYP	-1401.987	-1401.512	-1402.265	-5.523	-1.265	-4.256	13.087	14.189	19.303	2.991
HSEH1PBE	-1401.656	-1401.482	-1401.845	-4.254	-2.453	-3.002	9.396	7.187	11.829	0.549
HCTH407	-1401.438	-1401.236	-1401.654	-4.365	-2.688	-3.258	10.242	8.184	13.11	0.570
WB97XD	-1401.068	-1399.879	-1399.954	-4.675	-2.741	-3.784	25.645	35.093	43.465	1.043

Table 6. Electronic energies of the neutral, positive and negative molecular systems (in au), the HOMO, LUMO, and SOMO orbital energies (in eV), JI, JA, JHL, and ΔSL descriptors (also in eV) calculated with DFT/B3LYB, CAM-B3LYP, HSEH1PBE, HCTH407and WB97XD for compound P2

	E_o	E^+	E^-	HOMO	LUMO	SOMO	J_i	J_A	J_{HL}	ΔS_L
B3LYP	-1561.379	-1561.723	-1561.587	-5.358	-3.011	-4.022	11.017	6.349	12.715	0.991
CAM-B3LYP	-1561.164	-1561.023	-1561.364	-6.235	-1.998	-5.236	11.677	5.834	13.053	3.238
HSEH1PBE	-1560.886	-1560.736	-1561.087	-5.624	-3.225	-3.854	11.093	7.306	13.282	0.629
HCTH407	-1560.652	-1560.523	-1560.756	-5.864	-3.741	-4.056	8.693	7.251	11.32	0.315
WB97XD	-1560.365	-1560.254	-1560.546	-5.744	-3.994	-4.158	10.669	7.014	12.768	0.464

Table 7. Electronic energies of the neutral, positive and negative molecular systems (in au), the HOMO, LUMO, and SOMO orbital energies (in eV), JI, JA, JHL, and ΔSL descriptors (also in eV) calculated with DFT/B3LYB, CAM-B3LYP, HSEH1PBE, HCTH407 and WB97XD for compound P3

	E_o	E^+	E^-	HOMO	LUMO	SOMO	J_i	J_A	J_{HL}	ΔS_L
B3LYP	-1723.247	-1723.621	-1723.487	-5.082	-3.074	-4.179	11.612	7.102	13.612	1.105
CAM-B3LYP	-1723.087	-1723.456	-1723.254	-6.357	-1.023	-5.214	10.901	9.017	14.147	4.191
HSEH1PBE	-1722.874	-1723.145	-1723.183	-5.231	-2.987	-3.587	13.638	4.386	14.327	0.601
HCTH407	-1722.587	-1722.883	-1722.897	-5.876	-3.245	-4.011	14.311	4.809	15.097	0.766
WB97XD	-1722.752	-1722.741	-1722.756	-5.001	-3.667	-4.572	5.109	3.966	6.468	0.905

Table 8. Electronic energies of the neutral, positive and negative molecular systems (in au), the HOMO, LUMO, and SOMO orbital energies (in eV), JI, JA, JHL, and ΔSL descriptors (also in eV) calculated with DFT/B3LYB, CAM-B3LYP, HSEH1PBE, HCTH407 and WB97XD for compound P4

	E_o	E^+	E^-	HOMO	LUMO	SOMO	J_i	J_A	J_{HL}	ΔS_L
B3LYP	-1568.746	-1568.969	-1568.762	-4.009	-2.815	-3.219	4.444	3.252	5.507	0.404
CAM-B3LYP	-1568.523	-1568.621	-1568.587	-5.674	1.775	-4.236	7.415	4.441	8.643	2.461
HSEH1PBE	-1568.311	-	-	-4.236	-2.546	-3.578	6.303	0.474	6.321	1.032

		1568.422	1568.387							
HCTH407	-1568.186	-1568.321	-1567.265	-4.701	-2.312	-3.256	20.359	1.361	20.404	0.056
WB97XD	-1567.887	-1568.077	-1566.756	-4.887	-2.905	-3.876	25.887	2.264	25.986	0.971

Table 9. Electronic energies of the neutral, positive and negative molecular systems (in au), the HOMO, LUMO, and SOMO orbital energies (in eV), JI, JA, JHL, and ΔSL descriptors (also in eV) calculated with DFT/B3LYB, CAM-B3LYP, HSEH1PBE, HCTH407 and WB97XD for compound P5

	E_o	E^+	E^-	HOMO	LUMO	SOMO	J_i	J_A	J_{HL}	ΔS_L
B3LYP	-1528.419	-1528.845	-1528.689	-4.291	-3.059	-3.547	11.637	8.532	14.43	0.488
CAM-B3LYP	-1528.209	-1528.546	-1528.458	-3.256	-2.009	-2.658	10.031	7.16	12.324	0.649
HSEH1PBE	-1528.025	-1528.126	-1528.087	-4.215	-3.546	-3.951	5.902	0.797	5.955	0.405
HCTH407	-1527.886	-1528.056	-1527.911	-4.985	-3.987	-4.031	5.665	0.638	5.701	0.044
WB97XD	-1527.621	-1527.833	-1527.725	-5.023	-4.002	-4.552	7.852	1.766	8.049	0.550

Table 10. Electronic energies of the neutral, positive and negative molecular systems (in au), the HOMO, LUMO, and SOMO orbital energies (in eV), JI, JA, JHL, and ΔSL descriptors (also in eV) calculated with DFT/B3LYB, CAM-B3LYP, HSEH1PBE, HCTH407 and WB97XD for compound P6

	E_o	E^+	E^-	HOMO	LUMO	SOMO	J_i	J_A	J_{HL}	ΔS_L
B3LYP	-1515.384	-1515.786	-1515.548	-4.328	-3.243	-3.985	8.79	7.695	11.682	0.742
CAM-B3LYP	-1515.214	-1515.544	-1515.355	-4.008	-2.008	-3.879	7.844	6.971	10.494	1.871
HSEH1PBE	-1515.018	-1515.315	-1515.245	-3.987	-3.654	-3.801	10.163	4.427	11.086	0.147
HCTH407	-1514.857	-1515.095	-1514.953	-3.564	-3.874	-3.652	6.176	2.601	6.701	0.222
WB97XD	-1514.687	-1514.901	-1514.766	-3.148	-3.212	-3.012	5.297	2.61	5.906	0.201

The overall conclusion that can be extracted from the inspection of the results presented in Tables 5 to 10 is that in agreement with our previous studies on P1 to P6, the values of JI, JA, and JHL are actually not zero. Nevertheless, the results tend to be impressive especially for the CAM-B3LYB density functional. As well, the ΔSL descriptor reaches the minimum values when HSEH1PBE and HCTH107 density functional are used in the calculations. This implies that there are sufficient justifications to assume that the LUMO of the all products.

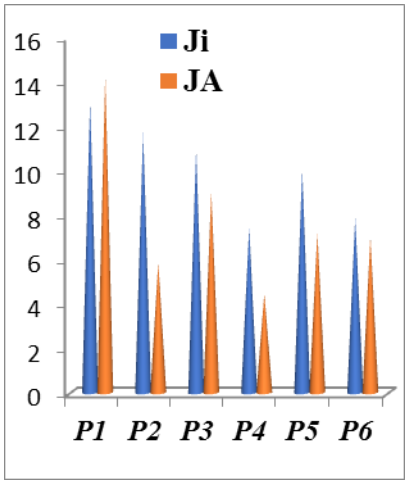

Fig. (4a)

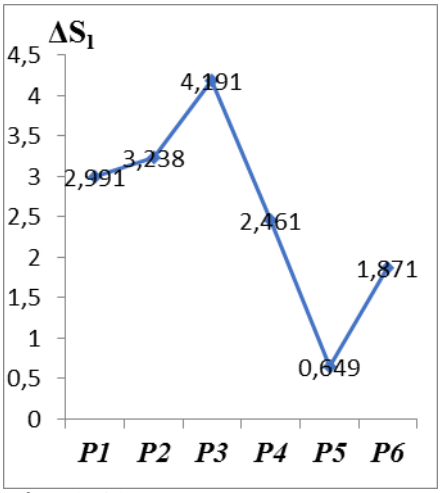

Fig. (4b)

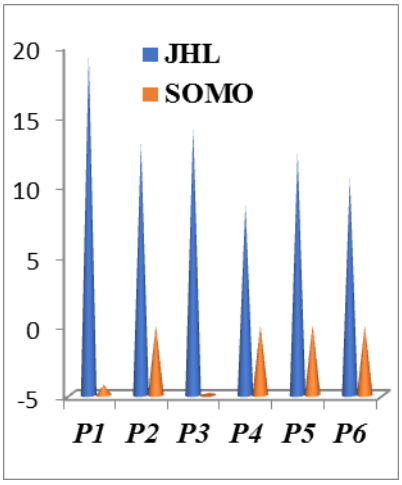

Fig. (4c)

Fig. 4. Plot of JA and JA descriptor (Figure 4a), ΔSL (Figure 4b), JHL and SOMO (Figure 4c) for compounds P1 to P6 by CAM-B3LYB

The values of *JI, JA*, and *JHL* are actually not zero. Nevertheless, the results tend to be impressive especially for the CAM-B3LYB density functional. As well, the ΔSL descriptor reaches the minimum values when HSEH1PBE and HCTH407 density functionals are used in the calculations. This implies that there are sufficient justifications to assume that the SOMO of the neutral approximates the electron affinity.

The analysis of the results given in (Tables 5 to 10) and (Figure 4) clearly shows in one hand that the JA and JA descriptor follows the order as $P_1 < P_3 < P_2 < P_5 < P_4 < P_6$ (Figure 4a). On the other hand, the ΔSL follows the stability is lowest for P3 and P2 products (Figure 4b).

4. Conclusion

In this paper, we have presented a new study performed on the chemical reactivity of P1 to P6 compounds on conceptual DFT as a tool to explain molecular interactions. The obtained results show that:

- The electron-accepting ability (ELUMO) is seen to follow the order as P6 < P3 < P5 < P2 < P4 < P1;
- (P4, P1, P5) and (P3, P6, P2) proudcuts show higher and lower DMTOTAL, respectively;
- The JA and JA descriptor follows the order as P1 < P3 < P2 < P5 < P4 < P6. On the other hand, the ΔSL follows the stability is lowest for P3 and P2 products.

5. Funding statement

This research did not receive any specific grant from funding agencies in the public, commercial, or not-for-profit sectors.

6. Conflict of interest

The authors declare no conflict of interest.

References

Aihara et al., 1999 - Aiharaб JıoI. (1999). Reduced HOMO-LUMO gap as an index of kinetic stability for polycyclic aromatic hydrocarbons. *J Phys Chem A*. 103: 7487-95.

Ameri, 2009 – *Ameri, T., Dennler, G., Lungen schmied, C., Brabec, C.* (2009). Organic solar cell design as a function of radiative quantum efficiency. *Energy Environ Sci.* 2: 347-363.

Bahadur, Srivastava, 2004 – *Bahadur, L., Srivastava, P.* (2004). Small molecular white organic light emitting devices with a single emission layer. *Semicond. Sci. Technol.* 19: 531.

Bahçeli et al., 2015 – *Avcı, D., Bahçeli, S., Tamer, Ö., Atalay, Y.* (2015). Comparative study of DFT/B3LYP, B3PW91, and HSEH1PBE methods applied to molecular structures and spectroscopic and electronic properties of flufenpyr and amipizone. *Can. J. Chem.* 93: 1147.

Becke, 1993 – *Becke, A.D.* (1993). A new mixing of Hartree-Fock and local density functional theories. *J. Chem. Phys.* 98: 1372.

Bhattacharjya et al., 2008 – *Jain, V., Rajbongshi, B.K., Tej Mallajosyula, A., Bhattacharjya, G., Iyer, S.S.K., Ramanathan, G.* (2008). Segregation into Chiral Enantiomeric Conformations of an Achiral Molecule by Concomitant Polymorphism. *Sol. Energy Mater. Sol. Cells*. 92 : 1043.

Boreland, 2008 – *Bagnall, D.M., Boreland, M.* (2008). Photovoltaic technologies. *Energy policy*. 36: 4390-4396.

Chen et al., 2017 – *Chen, L., Lu, J., Huang, T., Cai, Y.D.* (2017). A computational method for the identification of candidate drugs for non-small cell lung cancer. *PLoS One*. 12: e0183411.

Chuang et al., 2009 – *Chuang, W.T., Chen, B.S., Chen, K.Y., Hsieh, C.C., Chou, P.T.* (2009). Fluorescent protein red Kaede chromophore; one-step, high-yield synthesis and potential application for solar cells. *Chem. Commun.* 6982.

Desharnais et al., 2003 – *Boger, D.L., Desharnais, J., Capps, K.* (2003). Solution-phase combinatorial libraries: Modulating cellular signaling by targeting protein-protein or protein-DNA interactions. *Angew Chem Int Ed Engl.* 42: 4138-76.

El idrissi et al., 2019 – *Zeroual, A., Ríos-Gutiérrez, M., El Alaoui El Abdallaoui, H., Domingo L.R.* (2019). An MEDT study of the mechanism and selectivities of the [3 + 2] cycloaddition reaction of tomentosin with benzonitrile oxide. *Int J Quantum Chem*. 1(1): 1-9.

Francl, 1982 – *Francl, M.M., Pietro, W.J., Hehre, W.J.J.* (1982). Self-Consistent Molecular Orbital Methods. XXIII. A Polarization-Type Basis Set for Second-Row Elements. *Chem. Phys* .77: 3654-3665.

Frisch et al., 2009 – *Frisch, J., Trucks, G.W., Schlegel, H.B. et al.* (2009). Gaussian 09, Revision a.1, Gaussian, Inc., Wallingford, CT.

Ghanadzadeh et al., 2000 – *Ghanadzadeh, A., Ghanadzadeh, H., Ghasmi G.* (2000). On the molecular structure and aggregative properties of Sudan dyes in the anisotropic host. *J. Mol. Liq.* 88: 299-308.

Green et al., 2009 – *Green, M., Emery, K., Hishikawa, Y., Warta, W.* (2009). Solar Power Generation: Technology, New Concepts & Policy. *Prog Photovol Res Appl.* 17: 320-326.

Gupta et al., 2017 – *Ansary, I., Das, A., Gupta, P.S., Bandyopadhyay, A.K.* (2017). Synthesis, molecular modeling of N-acyl benzoazetinones and their docking simulation on fungal modeled target. *Synth Commun*. 47: 1375-1386.

Hadipour, 2008 – *Hadipour, A., de Boer, B., Blom, P.* (2008). Organic tandem and multi-junction solar cells. *Adv Funct Mater*. 18: 169-181.

Hansch et al., 2003 – *Hansch, C., Steinmetz, W.E., Leo, A.J., Mekapati, S.B., Kurup, A., Hoekman D.* (2003). On the role of polarizability in chemical-biological interactions. *J. Chem Inf Comput Sci*. 43: 120-5.

Harris et al., 1999 – *Harris, P.G., Baker, C.A., Green, K., Iaydjiev, P., Ivanov, S., May, D.J.* (1999). New experimental limit on the electric dipole moment of the neutron. *Phys Rev Lett*. 82: 904.

Hurst et al., 2000 – *Hurst, G.J., Dupuis, M., Clementi, E.* (2000). A binitio analytic polarizability, first and second hyperpolarizabilities of large conjugated organic molecules: Applications to polyenes C4H6 to C22H24. *J. Chem Phys*. 89: 385-95.

Kim et al., 2005 – *Reyes-Reyes, M., Kim, K., Carroll, D.* (2005). Origins of performance in fiber-based organic photovoltaics. *Appl Phys Lett*. 87: 083506.

Lee, 2007 – *Kim, J., Lee, K., Coates, N., Moses, D., Nguyen, T., Dante, M., Heeger, A.* (2007). Organic, Inorganic and Hybrid Solar Cells: Principles and hybrid Solar Cells. *Science*. 317: 222-225.

Lim et al., 1999 – *Lim, I.S., Pernpointner, M., Seth, M., Laerdahl, J.K., Schwerdtfeger, P., Neogrady, P.* (1999). Relativistic coupled-cluster static dipole polarizabilities of the alkali metals from Li to element 119. *Phys Rev A*. 60: 2822.

Lu et al., 2015 – *Lu, L., Kelly, M.A., You, W., Yu, L.* (2015). Status and prospects for ternary organic photovoltaics. *Nat. Phot.* 9: 491e500.

Obot et al., 2009 – *Obot, I.B., Obi-Egbedi, N.O., Umoren, S.A.* (2009). Antifungal drugs as corrosion inhibitors for aluminium in 0.1 M HCl. *Corrosion Science*. 51(8): 1868-75.

Park et al., 2009 – *Park, S., Roy, A., Beaupré, S., Cho, S., Coates, N.E., Moon, J., Moses, D., Leclerc, M., Lee, K., Heeger,* A. (2009). Polymer Photovoltaics: Materials, Physics and Device Enginee. *Nat. Photon*. 3: 297-302.

Pereira et al., 2017 – *Pereira, T.L., Leal, L.A., da Cunha, W.F., Timóteo de Sousa, R., Ribeiro Junior, L.A. et al.* (2017). Optimally tuned functionals improving the description of optical and electronic properties of the phthalocyanine molecule. *J. Mol. Model*. 23: 71.

Weigend et al., 2005 – *Weigend, F., Ahlrichs, R.* (2005). Balanced basis sets of split valence, triple zeta valence and quadruple zeta valence quality for H to Rn: design and assessment of accuracy. *Phys. Chem. Chem. Phys.* 7: 3297-3305.

Xue et al., 2004 – *Xue, Y., Li, Z.R., Yap, C.W., Sun, L.Z., Chen, X., Chen, Y.Z.* (2004). Effect of molecular descriptor feature selection in support vector machine classification of pharmacokinetic and toxicological properties of chemical agents. *J Chem Inf Comput Sci.* 44: 1630-8.

Yang et al., 2005 – *Ma, W., Yang, C., Gong, X., Lee, K., Heeger, A.* (2005). Thermally Stable, Efficient Polymer Solar Cells with Nanoscale Control of the Interpenetrating Network Morphology. *Adv Funct Mater*. 15: 1617-1622.

Yang, 1988 – *Lee, C.T., Yang, W.T, Parr, R.G.* (1988). Density-functional exchange energy approximation with correct asymptotic behavior. *Physical Review B.* (37): 785-89.

You et al., 2000 – *You, Y., He, Y., Burrows, P.E., Forrest, S.R., Petasis, N.A., Thompson, M.E.* (2000). Tuning the solid-state emission of the analogous GFP chromophore by varying alkyl chains in the imidazolinone ring. *Adv. Mater*. 12: 1678.

Zeroual et al., 2017 – *Zoubir, M., Zeroual, A., El Idrissi, M., Bkiri, F., Benharref, A., Mazoir, N., El Hajbi, A.* (2017). Experimental and theoretical analysis of the reactivity and regioselectivity in esterification reactions of diterpenes (totaradiol, totaratriol, hinikione and totarolone). *Mediterranean Journal of Chemistry*. 6(4): 98-107.

Zhan et al., 2003 – *Zhan, C.G., Nichols, J.A., Dixon, D.A.* (2003). Ionization potential, electron affinity, electronegativity, hardness, and electron excitation energy: Molecular properties from density functional theory orbital energies. *J. Phys Chem A*. 107: 4184-4195.

Zhang et al., 2007 – *Zhang, C., Song Y.L., Wang. X.* (2007). Correlations between molecular structures and third-order non-linear optical functions of heterothmetallic clusters: a comparative study. *Chem. Reviews*. 251: 1-2.